CONFERENCE PRE-PRINT

WEST LONG-PULSE ACHIEVEMENTS IN SUPPORT OF NEXT-STEP FUSION DEVICES

R. J. Dumont CEA, IRFM Saint-Paul-lez-Durance, France Email: remi.dumont@cea.fr

T. Fonghetti, P. Maget, P. Manas, J.-F. Artaud, C. Bourdelle, L. Colas, G. Ciraolo, Y. Corre, A. Ekedahl, N. Fedorczak, P. Forestier-Colleoni, A. Gallo, E. Geulin, B. Guillermin, C. Guillemaut, J. Garcia, J. P. Gunn, J. Hillairet, F. Imbeaux, E. Joffrin, X. Litaudon, D. Mazon, S. Mazzi, J. Morales, Ph. Moreau, R. Nouailletas, P. Puglia, C. Reux, N. Rivals, Y. Savoye-Peysson, E. Tsitrone, S. Vartanian CEA, IRFM Saint-Paul-lez-Durance, France

T. Barbui, L. F. Delgado-Aparicio, Princeton Plasma Physics Laboratory Princeton, NJ, USA

J. Gaspar, E. Vergnaud Aix Marseille Univ. Marseille, France

A. Grosjean University of Tennessee Knoxville, TN, USA

J. Huang, M. Li Institute of Plasma Physics, Chinese Academy of Sciences Hefei Anhui, P. R. China

E. Lerche LPP-ERM-KMS, Association EUROFUSION-Belgian State, TEC partner Brussels, Belgium

The WEST team#

#See http://west.cea.fr/WESTteam

The EUROfusion Tokamak Exploitation team##
##See the author list of E. Joffrin et al 2024 Nucl. Fusion **64** 112019

Abstract

The WEST superconducting tokamak, featuring a full tungsten environment and equipped with an actively cooled ITER-grade divertor, provides valuable inputs for future ITER operation. One of its distinctive features is that auxiliary plasma heating and current drive is exclusively supplied by radiofrequency systems. Scenario development supported by integrated modelling has allowed pulses exceeding 22 min and 2.6 GJ of energy to be performed, based on feedback-controlled plasma current sustained by Lower Hybrid Current Drive power in order to achieve a zero-loop voltage target. This contribution describes the predict-first integrated modelling approach that has been employed in the context of this long-pulse scenario development endeavour, reviews the main achievements and the physics analyses performed, and draws prospects for further developments.

1. INTRODUCTION

WEST is a tokamak equipped with an actively cooled ITER-grade tungsten (W) divertor, as well as a superconducting toroidal magnetic field system producing a magnetic field up to $B_0\sim3.7$ T at major radius $R_0\sim2.5$ m (typical minor radius $a_0\sim0.5$ m). Several plasma configurations (lower/upper X-point, double-null) allow various aspects related to the operation of future magnetic fusion devices, including ITER, to be explored [1].

Among these aspects, preparing for long pulse operation (LPO), i.e., performing discharges with durations well above the plasma confinement time and reaching plasma-wall interaction timescales, is crucial in the context of developing fusion-based power plants [2].

One of the distinctive features of the WEST tokamak is that the auxiliary power for plasma heating and current drive is exclusively supplied by radiofrequency (RF) sources. Its Lower Hybrid Current Drive (LHCD) system consists of two antennas: a fully-active (resp. passive-active) multijunction launcher able to provide up to 4 MW (resp. 3 MW) power and drive the plasma current (up to $I_p\sim1$ MA) in continuous wave (CW) conditions, at frequency 3.7 GHz. An Ion Cyclotron Resonance Frequency (ICRF) system is also available, capable of coupling up to 9 MW during 30 s or up to 3 MW during 1000 s, in frequency range 48-63 MHz. Finally, an Electron Cyclotron Resonance Heating (ECRH)/Current Drive (ECCD) system has been commissioned in WEST [3]. At frequency 105 GHz, it can supply up to 1 MW in 2025, and the power level is expected to reach 3 MW in 2026. As such, RF power input in WEST plasmas results in dominant electron heating, in part as a result of the D(H) minority scheme typically used for Ion Cyclotron Resonance Heating (ICRH) [4], and low torque injection. This coincides with expectations for ITER, in which large EC power and high-energy NBI power induce dominant electron heating with relatively modest momentum input [5].

We report here on recent achievements related to the development of steady-state discharges in WEST. In Section 2 is illustrated the method used to develop LHCD-only discharges, based on extensive integrated modelling. Section 3 is devoted to the description of achievements related to long pulses in the campaigns performed between 2023 and 2025. In section 4, the status of physics analyses of the pulses performed is presented. Finally, in section 5, prospects in terms of future LPO developments in WEST, are underlined.

2. LONG PULSE SCENARIO DEVELOPMENT BASED ON INTEGRATED MODELLING

Developing long pulses in tokamaks requires achieving conditions with low, or even possibly zero, loop voltage, V_{loop} . This implies that the plasma current must be sustained by non-inductive means. In WEST, up until now, the non-inductive current has consisted of a bootstrap contribution, supplemented by LH-driven current. Upon application of the LHCD power (P_{LHCD}), the drop in loop voltage $\Delta V \equiv V_{LHCD}$ - V_{Ω} (V_{Ω} is the loop voltage in the ohmic phase, whereas V_{LHCD} is the loop voltage after the RF application) can be related to the bootstrap fraction f_{bs} and the LHCD efficiency, η_{LH} , by the following, simplified, relation [6,7]

$$-\frac{\Delta V}{V_{\Omega}} = \frac{V_{\Omega} - V_{LHCD}}{V_{\Omega}} = f_{bs} + \eta_{LHCD} \frac{P_{LHCD}}{\overline{n_1}RI_p},$$

where R is the major radius, \overline{n}_l is the central line-averaged electron density. As a result, non-inductive operation, corresponding to $-\Delta V/V_{\Omega}=1$, can be approached by increasing the LHCD power and/or decreasing the plasma density or current. It was shown in a multi-machine study that the LHCD efficiency, η_{LHCD} , is adequately fitted

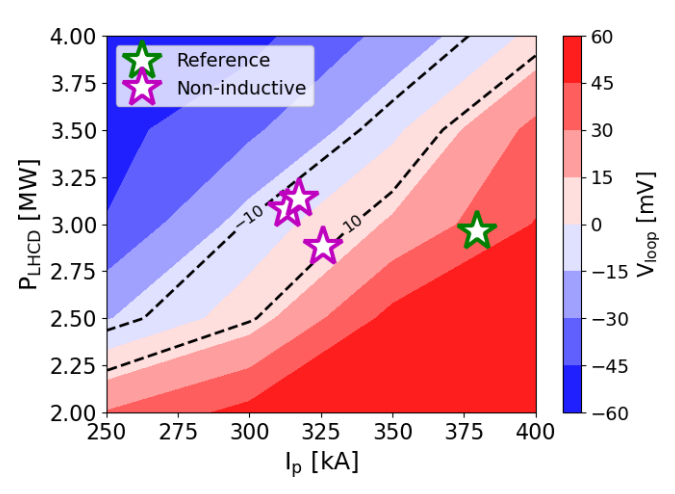


Figure 1: Parameter range for non-inductive operation in WEST. The loop voltage predicted by HFPS simulations is shown in color scale, with the ± 10 mV domain delimited by dashed lines. The reference pulse (57757) is shown as a green star, whereas three non-inductive pulses (59182, 59309, 59310) appear as magenta stars.

by a function proportional to $\tau_E{}^{0.4},$ with τ_E the energy confinement time (see Ref. [8] and references therein). This makes the picture more complex, as confinement tends to increase with current and density. Indeed, plasma confinement in discharges in which the current profile is mainly determined by the LHCD system results from a complex, non-linear, interplay between power sources, current diffusion, particle and heat transport, etc... To simulate these effects in a selfconsistent fashion, the High-Fidelity Plasma Simulator (HFPS), an IMAS version of the JINTRAC/JETTO framework has been used. As extensively described in Ref. [8], for the purpose of adequately describing these pulses, it is essential to couple a model for LHCD physics and a quasilinear turbulent transport model. For the latter, TGFL-sat2 has been used to predict heat and particle turbulent fluxes up to the plasma separatrix. WEST discharge 57757, lasting 101 s and featuring loop voltage V_{loop}~47 mV has been used as a reference. After a thorough validation,

several scans have been performed to identify the changes in parameters required to lower this value until quasi

or fully non-inductive conditions were obtained, as shown in Figure 1. Additional boundaries are set by various physical or technological constraints. An example of the latter is the fact that WEST being a fully actively cooled device, water pipes are installed in the upper part of the vacuum vessel to ensure the cooling of electron ripple protection elements, placing effective restrictions in terms of current/density/LHCD power. Another important aspect is that non-inductive discharges are challenging from an MHD stability standpoint. Reversed safety factor (q) profiles typical of LHCD-dominated discharges are known to be prone to the destabilization of tearing modes [9]. It should be mentioned that the MHD stability of these pulses is investigated a posteriori. The stability calculations clearly show that increasing LHCD powers and/or decreasing plasma currents induces more reversed q-profiles that tend to be problematic from a stability standpoint.

3. LONG PULSE ACHIEVEMENTS

This extensive simulation effort has resulted in the successful achievements of many noninductive, L-mode, discharges in WEST during experimental campaigns performed between 2023 and 2025. This is summarized in Figure 3. Twenty discharges have exceeded 200 s. It must be stressed that no boronization or specific conditioning has been employed prior to these experimental sessions. During this effort, several scenarios have been developed. All were based on a double feedback control scheme, with a fixed value imposed for V_{loop} by the central solenoid coil voltage, and Ip maintained to its prescribed value by the LHCD power. On the basis of further predictive simulations performed using the HFPS, scenarios at I_p~0.27 MA have been developed, using a combination of the two LHCD antennas to couple a total power in the range ~3-3.5 MW to the plasma. The lineaveraged central density is $\overline{n}_1 \sim 3 \times 10^{19}$ m⁻³. A pulse performed in this parameter range, 59763, is shown in Figure 2 (left).

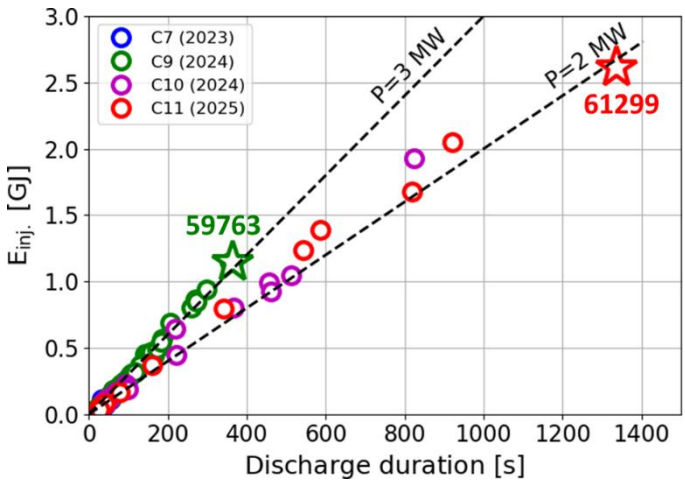


Figure 3: Energy vs discharge duration in the course of long pulse scenario developments performed in WEST during the 2023-2025 period campaigns. Each symbol corresponds to a long-duration pulse. The two diagonal dashed lines denote operation at average RF power 3 MW and 2 MW. Two pulses discussed in the main text, 59763 and 61299, are highlighted.

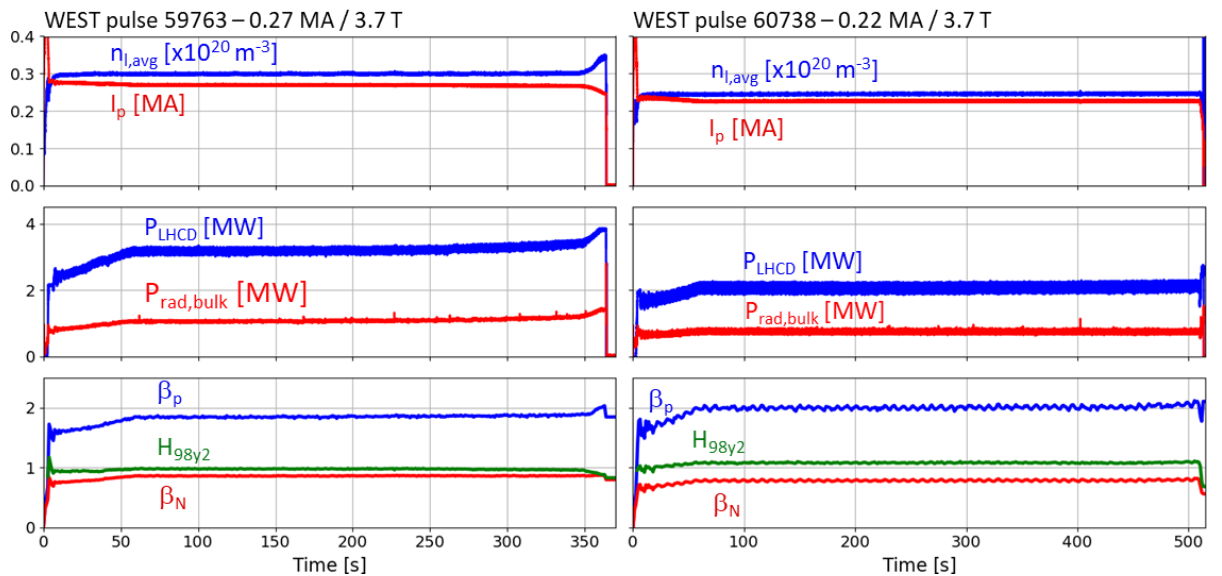


Figure 2: Time traces of WEST pulses 59763 (left) and 60738 (right). From top to bottom: line-averaged central density, plasma current, LHCD power, radiated power (bulk), poloidal beta β_P , confinement factor H_{98y2}, normalized toroidal beta β_N . The loop voltage was set to 3 mV. The duration in this case is 364 s with an energy of 1.15 GJ. The central electron

The loop voltage was set to 3 mV. The duration in this case is 364 s with an energy of 1.15 GJ. The central electron temperature is $T_{e0}\sim4.3$ keV, poloidal beta $\beta_{P}\sim1.9$, normalized toroidal beta $\beta_{N}\sim0.9$ and confinement factor $H_{98y2}\sim1.1$ It should be recalled that although the latter is more relevant to H modes, it has been shown in the past that the

ITER H98 H-mode scaling law, when compared to the L-mode scaling law ITER L96, exhibits an opposite-sign exponent with respect to the aspect ratio. Since WEST is characterized by a large aspect ratio ($R_0/a_0 \sim 5-6$), both scaling laws tend to converge to similar H factor values [10]. This pulse, as well as other long pulses performed in the attached divertor regime in WEST, are characterized by the presence of intermittent UFOs [11], with usually only transient impacts on the radiated power and other plasma quantities as a result of the reduction of the incoming W flux [12]. On the other hand, it can be seen that the density increases progressively in this pulse, impacting the LHCD efficiency. This increase is adequately compensated by an increase of the LHCD power until it becomes significantly more pronounced after t~300 s, inducing a decrease of I_p and a subsequent MHD crash. This density increase has been attributed to the outgassing of far-off elements in the vacuum vessel, still to be precisely identified. It must be mentioned that the repetition of pulses has allowed to demonstrate that a progressive conditioning was occurring, as the onset of outgassing was progressively observed later in the pulses. However, the conditioning rate observed would have required the repetition of many long pulses, incompatible with the allocated experimental time for these developments. As a result, new simulations have been performed to identify parameters corresponding to a lower LHCD power request. It was established that operating at reduced current, $I_p \sim 0.22$ MA, and corresponding reduced density, $\overline{n}_1 \sim 2.4 \times 10^{19}$ m⁻³, would require a LHCD power in the range 2-2.5 MW, i.e., substantially lower than in the case of pulse 59763. Several long pulses have been successfully performed in this regime, with loop voltage V_{loop}=3 mV, and using a combination of the two LHCD launchers. An example, WEST pulse 60738, is shown in Figure 2 (right). It is characterized by a LHCD power in the 2-2.2 MW range to sustain the plasma current, as expected from modelling. Central electron temperature is $T_{e0} \sim 3.4 \text{ keV}$, poloidal beta $\beta_p \sim 2.0$, normalized toroidal beta $\beta_N \sim 0.8$, and confinement factor $H_{98v2} \sim 1.1$. As other non-inductive pulses typical of these developments, this discharge appears to be resilient to external perturbations such as UFOs, and was terminated because of an LHCD power fault. On the other hand, it does not exhibit the same outgassing phenomenon as pulse 59763.

Further analyses have shown that even in the absence of this unexpected technical failure of the LHCD system, this type of pulse could not have lasted more than ~860 s because of limitations in the capabilities of the RF plant main cooling loop. Remedial measures to overcome this problem could be implemented only after the WEST campaign. Rather than using a combination of the two LH antennas, it was therefore decided to perform pulses with only the fully-active multi-junction coupler (LH1). This has been successful since pulse 61299, performed with hydrogen gas fuelling during the C11 campaign in 2025, with a duration of 1337 s, displays an energy injected/extracted reaching 2.61 GJ, constituting the duration and energy record to date for WEST. It is shown in

Figure 4. Although the parameters (plasma current, density, LH power requested) are similar to those of pulse 60738, shown in Figure 2 (right), several differences between these two pulses can be noted. Firstly, in pulse 61299, the loop voltage request has been strictly set to zero, making it a fully noninductive pulse. Secondly, a klystron fails at t~75 s, which results somewhat surprisingly in a subsequent decrease of the power request. This has been attributed to differences in the toroidal spectrum, resulting in an overall improved LHCD efficiency. Another difference is that this pulse is characterized by the presence of mild MHD activity, absent from pulses 59763 and 60738. In this discharge, the MHD activity results in intermittent changes of regime, e.g., in the period t~200-400 s, accompanied by adaptations of the LH power from the controller to compensate for the modified efficiency. A second klystron failure occurs at t~1040 s, and induces a change towards a regime characterized by more pronounced relaxations. Although the MHD activity observed does not impact the LHCD efficiency in a drastic way (the total LH power level remaining

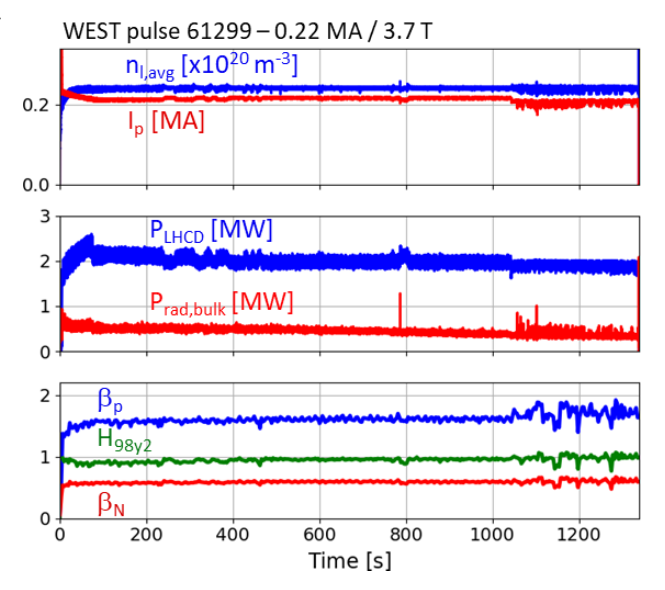


Figure 4: Time traces of record WEST pulse 61299. From top to bottom: line-averaged central density, plasma current, LHCD power, radiated power (bulk), poloidal beta β_P , confinement factor H_{98y2} , normalized toroidal beta β_N .

comparable to its value in pulse 60738), the global confinement is impacted. Indeed, as shown in the bottom panel of Figure 4, $\beta_p \sim 1.6$, $\beta_N \sim 0.6$, and $H_{98y2} \sim 0.9$, i.e., lower values compared to pulse 60738. It must be mentioned that although pulse 61299 has been performed in hydrogen, several similar pulses have been performed in deuterium. Pulse 61320, for instance, is a 921 s D₂ pulse displaying features very similar to pulse 61299, i.e., the presence of mild MHD activity and a confinement characterized by $\beta_p \sim 1.7$, $\beta_N \sim 0.6$, and $H_{98y2} \sim 0.8$.

4. PHYSICS ANALYSIS OF LONG PULSES PERFORMED IN WEST

A global study of the pulses performed in the framework of this effort has been conducted. To achieve this, the method and tools described in Section 2.1 of Ref. [13] are used. A reduced database is constructed by selecting

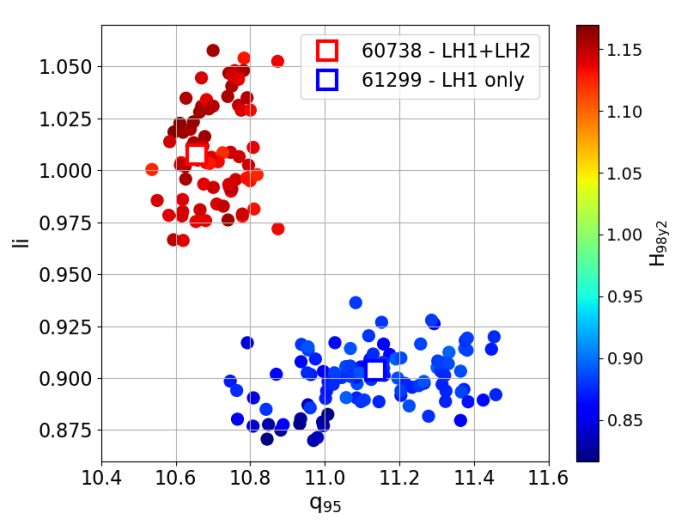


Figure 6: H_{98y2} confinement factor (color scale) vs safety factor profile value at normalized radius 0.95 (q₉₅) and plasma internal inductance (li). The two pulses discussed in the main text, 60738 and 61299, are highlighted.

time periods (plateaus) during which the various plasma quantities are stationary. In this case, all pulses performed in the experimental session devoted to long pulse developments have been considered, with a filter imposing I_p≥0.2 MA, $V_{loop} \le 10 \text{ mV}$ and $\Delta t_{min} = 2 \text{ s}$, with Δt_{min} the minimum acceptable duration for a given plateau. Such a filter allows all transient states to be ignored. In Figure 6 is displayed the confinement factor, H_{98y2} in color scale in the (q₉₅, li) domain, with q95 the value of q at normalized radius ρ =0.95, and li the plasma internal inductance. These quantities are provided by the equilibrium code NICE [14] constrained by polarimetry measurements. The two classes of pulses discussed previously appear clearly, and are linked to differences between the current profiles when only the LH1 coupler is used or when the two couplers (LH1 + LH2) are employed. Peaked current profiles (corresponding to larger values of li) are accompanied by better confinement. This

difference in current profiles is confirmed by hard X-ray (HXR) emission profiles, which are measured by the horizontal camera installed in WEST. Pulse 60738 is characterized by a larger HXR peaking, compared to pulse 61299. This is consistent with the equilibrium reconstruction performed using NICE, which yields a current profile for pulse 61299 broader than its counterpart for pulse 60738. These differences in current profiles can be linked to differences in the LH deposition profile and/or the loss of energetic electrons caused by the presence of MHD activity [15].

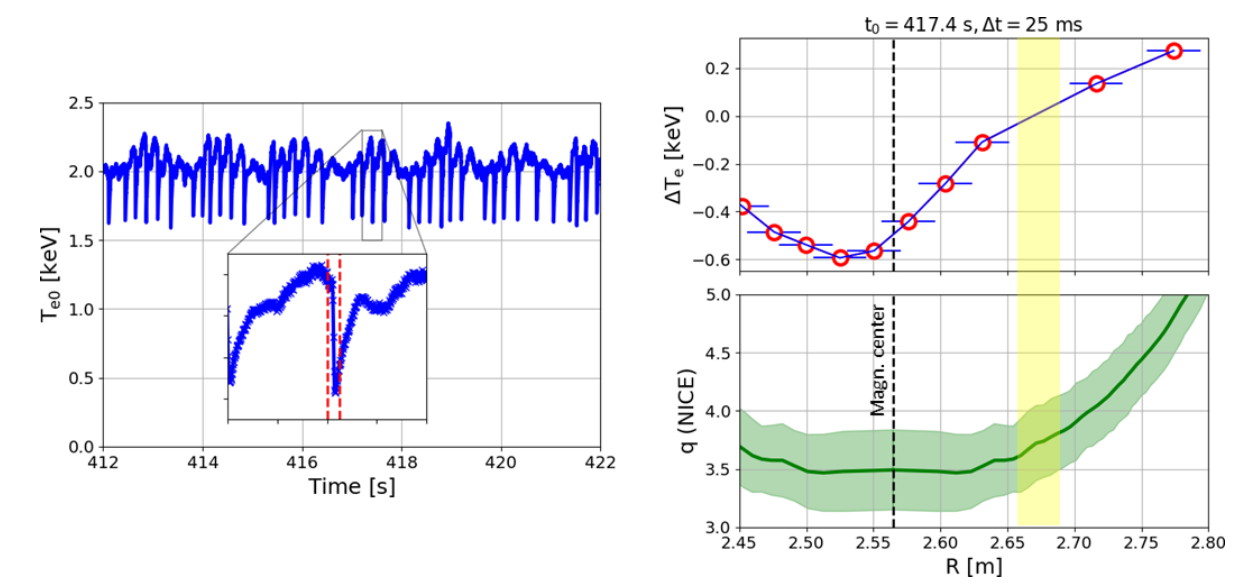


Figure 5: Periodic crashes of electron temperature in WEST pulse 61320 (left). Difference in ECE electron temperature profile after and before crash (top right). The approximate inversion radius is denoted by the yellow area. The q profile from NICE, averaged over 5 s is shown in the bottom right figure, with reconstruction uncertainties represented by the shaded area.

An important difference between the two classes of pulses is the presence of mild MHD. Discharges with lower confinement display a mode at frequency ~0.8 kHz, accompanied by periodic relaxations of the electron temperature. These relaxations have been analysed using the magnetic diagnostics and the 32-channel ECE radiometer installed in WEST. In the pulses exhibiting mild MHD activity, the Mirnov coil measurements show that this mode is characterized by toroidal mode n=1, and poloidal modes m=3 and/or 4 (the data analysis for the m-number does not allow this uncertainty to be unambiguously lifted). The time trace of the central electron

temperature in the case of pulse 61320 is shown in Figure 5 (left). An analysis of the periodic crashes show that they are characterized by an inversion radius $R_{\rm inv}$ ~2.6-2.7 m, as depicted in Figure 5 (top right). The q-profile computed by NICE [13] constrained by polarimetry measurements at this time is shown in Figure 5 (bottom right). In these pulses, the analysis of fast acquisition (1 MHz) ECE data shows two magnetic islands developing before the crash, with opposite m-parities. Given the uncertainties on the precise value of q in the plasma core and the 1.5-2 cm uncertainty on the ECE measurement location, this is consistent with the interaction of two modes on q=3/1 and q=4/1, both at frequency f~0.8 kHz, followed by a magnetic reconnection on the q=4 surface. This is believed to be the cause for the crashes observed in pulses using LH1 only, and for the degraded confinement.

5. PROSPECTS FOR LONG PULSE DEVELOPMENT IN WEST

Efforts are underway to widen the range of application and increase the performance of long pulses in WEST. Operating at larger densities is expected to have a favourable impact on the plasma performance, by broadening the LHCD power deposition/current profile [17]. This has been tested by performing increasing density plateaux during pulses. An illustration is shown in Figure 7, for WEST pulse 61978, a fully non-inductive discharge. These pulses are characterized by the same mild MHD activity as described previously. Unsurprisingly, the LH power required to sustain the requested plasma current (0.23 MA) increases linearly with density. It is also observed that the plasma performance increases linearly with density (see Figure 7, right). This prospect will be investigated further in the near future, taking into account the progress made in the precise determination of the parameter domain relevant to LHCD discharges in WEST [17].

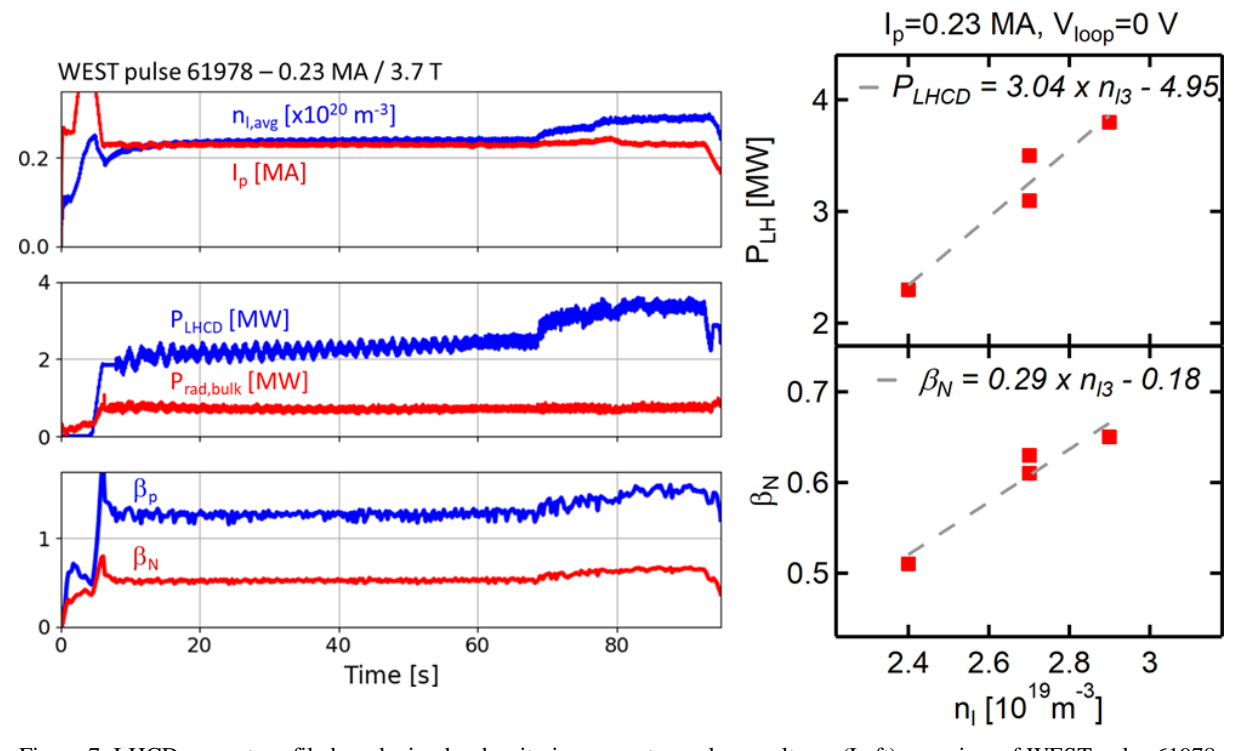


Figure 7: LHCD current profile broadening by density increase at zero loop voltage. (Left) overview of WEST pulse 61978. From top to bottom: line-averaged central density, plasma current, LHCD power, radiated power (bulk), poloidal beta β_{P} , confinement factor H_{98y2} , normalized toroidal beta β_{N} . (Top right) LHCD power required to sustain the plasma current versus density; (bottom right) normalized toroidal beta versus density.

Another possibility is to use the ICRF system, especially since ICRH has been shown to have a positive impact on non-inductive discharges performed using this system in conjunction with LHCD power in Tore Supra [18]. In the full tungsten environment of WEST, this has proven challenging so far, as the use of ICRH power typically requires a larger density, and is often associated with radiative collapses [19], related in part to the off-axis nature of the LHCD deposition profile [13]. The availability of EC power will facilitate the development of these scenarios, as localized core electron heating is expected to counteract the central radiation and anchor the LHCD deposition to the plasma centre [20, 21, 22]. Generally, integrated modelling predicts that compared to increasing the LH power, using a combination of LH and EC power will have a positive effect on energy confinement, and minimize the onset of MHD instabilities [8]. An illustration of this point appears in Figure 8, showing HFPS simulations of fully non-inductive WEST pulses in which the impact of additional on-axis ECCD on top of 2 MW of LHCD (orange) is compared to LHCD-only references (blue). As I_p is set to 300 kA, the non-inductive current

increases as the power (LH and/or EC) increases. It can be seen that ECCD is potentially beneficial for energy confinement (Figure 8, left panel) and is expected to minimise the triggering of MHD instabilities by controlling the q-profile reversal (Figure 8, right panel).

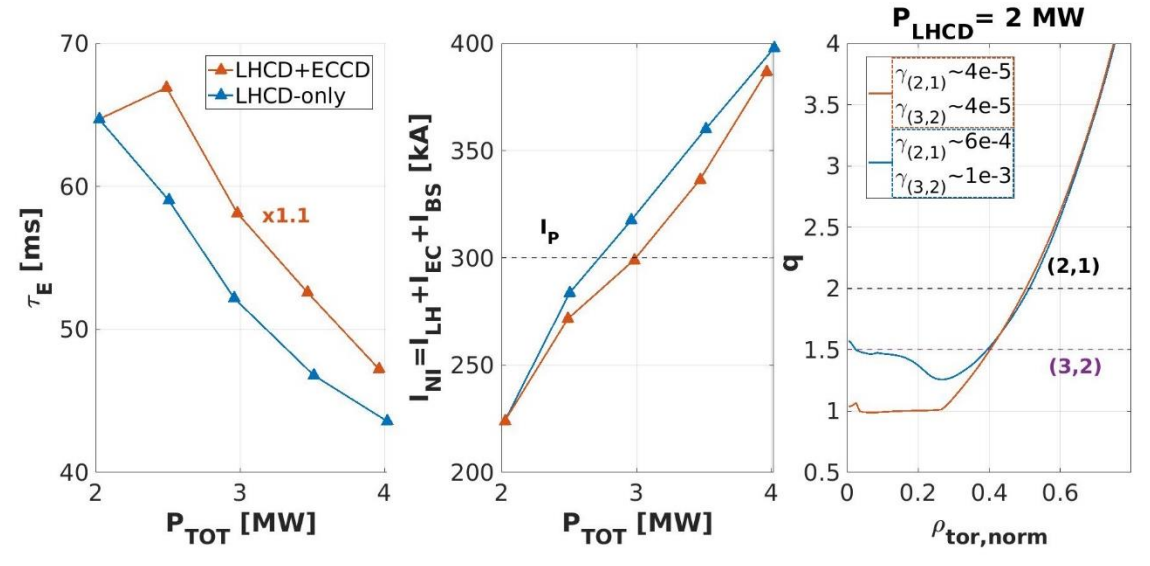


Figure 8: influence of central ECCD in WEST discharges at plasma current Ip=300 kA with LHCD power only (blue), and combined LHCD+EC power (orange). (Left) Energy confinement time; (center) non-inductive current; (right) q-profile, with the growth rate of the main tearing modes expected to be present in these conditions shown in the inset.

Finally, whereas the pulses shown so far are all characterized by attached divertor conditions, with the electron

temperature on the inner (resp. outer) strike point of the order of 15 eV (resp. 20 eV), it is important to develop future fusion-device relevant scenarios in detached divertor conditions. Pulses in X-point radiator (XPR) regime have been successfully developed in WEST [23]. The conditions for the onset of the XPR are not obviously aligned with the conditions for long pulses. As a result, zero loop voltage scenarios in the XPR regime have to be specifically designed. So far, ~40-45 s pulses have been obtained, with loop voltages V_{loop}~150 mV. The N₂ injection required to sustain the XPR regime has to be thoroughly adjusted. Figure 9 shows an overview of pulse 62234, which is representative of these achievements. This pulse is characterized by poloidal beta $\beta_p \sim 1.3$, normalized toroidal beta β_N ~0.9, and confinement factor H_{98v2}~0.9, i.e., comparable to standard attached long pulses. On the other hand, the electron temperature on the inner (resp. outer) strike point is ~3.5 eV (~2 eV), i.e., much lower than in attached conditions, which is expected to have a positive impact on the scenario by mitigating lower divertor impurity sources. These developments will be pursued in the near future, and it is expected that the availability of EC power will allow the parameter range and overall performance to be further improved.

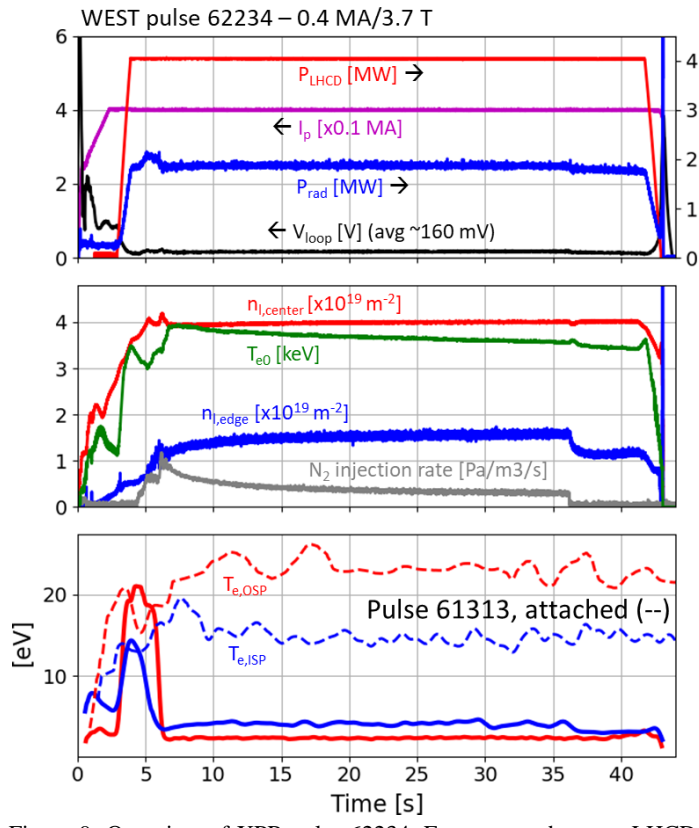


Figure 9: Overview of XPR pulse 62234. From top to bottom: LHCD power, plasma current, radiated power, loop voltage, line-integrated central density, central electron temperature, line-integrated edge density, N₂ injection rate. The bottom panel displays the electron temperature on the inner (resp. outer) divertor strike point compared to the same quantity in attached pulse 61313.

ACKNOWLEDGEMENTS

This work has been carried out within the framework of the EUROfusion Consortium, funded by the European Union via the Euratom Research and Training Programme (Grant Agreement No 101052200 - EUROfusion). Views and opinions expressed are however those of the author(s) only and do not necessarily reflect those of the European Union or the European Commission. Neither the European Union nor the European Commission can be held responsible for them.

REFERENCES

- [1] BUCALOSSI, J., et al., WEST full tungsten operation with an ITER grade divertor, Nucl. Fusion 64 11 (2024) 112022.
- [2] LITAUDON, X., et al., Long plasma duration operation analyses with an international multi-machine (tokamaks and stellarators) database, Nucl. Fusion **64** 1 (2024) 015001.
- [3] DELPECH, L., et al.., A new 3 MW ECRH system at 105 GHz for WEST, Fusion. Eng. Des. 186 (2023) 113360.
- [4] BOURDELLE, C., et al., WEST Physics Basis, Nucl. Fusion 55 6 (2015) 063017.
- [5] PITTS, R., et al., Plasma-wall interaction impact of the ITER re-baseline, Nucl. Mater. Energy 42 (2025) 101854.
- [6] GIRUZZI, G., et al., Measurement of the hot electrical conductivity in the PBX-M tokamak, Nucl. Fusion 37 (1997) 673.
- [7] GONICHE, M., et al., Advances in long pulse operation at high radio frequency power in Tore Supra, Phys. Plasmas **21** (2014) 061515.
- [8] FONGHETTI, T., et al., WEST L-mode record long pulses guided by predictions using Integrated Modeling, Nucl. Fusion **65** 5 (2025) 056018.
- [9] MAGET, P., et al., MHD activity in Tore Supra gigajoule scenario, Nucl. Fusion 44 (2004) 443.
- [10] BOURDELLE, C., et al., Ramping up RF power and increasing pulse length in the full tungsten environment of WEST, 46th EPS Conference on Plasma Physics (2019).
- [11] GASPAR, J. et al., Thermal and statistical analysis of the high-Z tungsten-based UFOs observed during the first deuterium high fluence campaign of the WEST tokamak, Nucl. Mater. Energy **41** (2024) 101745.
- [12] MAGET, P., et al., Tungsten control in long pulse operation: feedback from WEST to ITER, Plasma Phys. Control. Fusion **67** (2025) 045005.
- [13] OSTUNI, V., et al., Core radiative collapse characterisation and integrated modelling in WEST plasmas, Nucl. Fusion **62** (2022) 106034.
- [14] FAUGERAS, B., An overview of the numerical methods for tokamak plasma equilibrium computation implemented in the NICE code, Fusion Eng. Des. **160** (2020) 112020.
- [15] PEYSSON, Y., et al., Progress towards high-power lower hybrid current drive in TORE SUPRA, Plasma Phys. Control. Fusion **42** (2000) B87.
- [16] GAROFALO, A., et al., Development of high poloidal beta, steady-state scenario with ITER-like tungsten divertor on EAST, Nucl. Fusion **57** (2017) 076037.
- [17] MORALES, J., et al., Operational space for lower hybrid heating scenarios in the full tungsten environment of WEST, Nucl. Fusion **65** (2025) 106003.
- [18] DUMONT, R. J., et al., Multi-megawatt, gigajoule plasma operation in Tore Supra, Plasma Phys. Control. Fusion **56** (2014) 075020.
- [19] MAGET, P., et al., Tungsten accumulation during ion cyclotron resonance heating operation on WEST, Plasma Phys. Control. Fusion **65** (2023) 125009.
- [20] DU, H., et al., Analysis of performance degradation in an electron heating dominant H-mode plasma after ECRH termination in EAST, Nucl. Fusion **58** (2018) 066011.
- [21] LI, M. H., et al., Plasma heating by electron cyclotron wave and the temperature effects on lower hybrid current drive on EAST, Nucl. Fusion **63** (2023) 046019.
- [22] DUMONT, R. J., et al., RF power experiments in WEST to prepare for next-step fusion device operation, EPJ web conf. submitted (2025)
- [23] RIVALS, N., Experiments and SOLEDGE3X modeling of dissipative divertor and X-point Radiator regimes in WEST, Nucl. Mater. Energy **40** (2024) 101723.